Published in final edited form as:
Birth Defects Res A Clin Mol Teratol. 2012 March ; 94(3): 162–175. doi:10.1002/bdra.22890.

STRAIN-SPECIFIC MODIFIER GENES GOVERNING CRANIOFACIAL PHENOTYPES

Partha Mukhopadhyay, **Guy Brock**, **Cynthia Webb**, **M. Michele Pisano**, and **Robert M Greene**
University of Louisville Birth Defects Center, Department of Molecular, Cellular and Craniofacial Biology, ULSD, University of Louisville, Louisville, KY 40292

Abstract

BACKGROUND—The presence of strain-specific modifier genes is known to modulate the phenotype and pathophysiology of mice harboring genetically engineered mutations. Thus, identification of genetic modifier genes is requisite to understanding control of phenotypic expression. c-Ski is a transcriptional regulator. *Ski*$^{-/-}$ mice on a C57BL6J (B6) background exhibit facial clefting, while *Ski*$^{-/-}$ mice on a 129P3 (129) background present with exencephaly.

METHODS—In the present study, oligonucleotide-based gene expression profiling was utilized to identify potential strain-specific modifier gene candidates present in wild-type mice of B6 and 129 genetic backgrounds. Changes in gene expression were verified by TaqMan quantitative real-time PCR.

RESULTS—Steady-state levels of 89 genes demonstrated a significantly higher level of expression**,** and those of 68 genes demonstrated a significantly lower level of expression in the developing neural tubes from E8.5, B6 embryos when compared to expression levels in neural tubes derived from E8.5, 129 embryos.

CONCLUSIONS—Based on the results from the current comparative microarray study, and taking into consideration a number of relevant published reports, several potential strain-specific gene candidates, likely to modify the craniofacial phenotypes in various knockout mouse models have been identified.

Keywords

Neural tube; embryo; mouse; modifier gene; microarray

INTRODUCTION

The phenotype and pathophysiology of mice harboring genetically engineered mutations are frequently governed by the presence of strain-specific modifier genes (Sanford et al., 2001; Gerlai et al., 1996). Despite the existence of an identical complement of genes in all mouse strains, allelic variation and interactions between allelic variants may profoundly affect phenotype. Thus, determination of genetic modifier genes, and their expression patterns, is essential to understanding control of phenotypic expression.

Previous studies have documented that such “modifier” genes can dramatically affect phenotype. For example, a wide range of phenotypic variations can result from deletion of the p53 tumor suppressor gene (Donehower et al., 1995). Mutation of this gene in mice

Author to whom correspondence should be addressed: M. Michele Pisano, Ph.D., Birth Defects Center, University of Louisville, ULSD, 501 S. Preston Street, Suite 301, Louisville, KY 40292, Phone: (502) 852-1962 Fax: (502) 852-4702, drmikeky@gmail.com.

triggers a striking enhancement of tumorigenesis but the types and numbers of tumor formed as well as the age of tumor inception is dependent upon the genetic background on which the mutation is maintained (Harvey et al., 1993; van Meyel et al., 1998). Genetic background also affects the reproductive ability of leptin-deficient obese mice (Ewart-Toland et al., 1999). Moreover, embryonic survival and severity of cardiac and craniofacial defects have been shown to be affected by genetic background in fibroblast growth factor-16 null mice (Lu et al., 2010). Experimental evidences documented altered sensitivity to excitotoxic cell death between C57BL/6J and 129S6/S(v)E(v) mouse strains due to strain-dependent differences in cell surface receptor expression levels (Finn et al., 2010). Effect of genetic background on acoustic startle response in fragile X knockout mice has also been reported highlighting the influence of modifier genes on the fragile X phenotype (Errijgers et al., 2008). In transgenic and gene-targeted animals**,** a host of other physiologic endpoints including organ structure, locomotor activity, cardiovascular physiology, behavior, sepsis, ethanol tolerance and autoimmune susceptibility are influenced by genetic background (Aziz et al., 2007; Linsenbardt et al., 2009; Choi and Klingensmith, 2009; de Mooij-van Malsen et al., 2009; Shah et al., 2010; Painsipp et al., 2011; Boross et al., 2011).

The transcriptional regulator c-Ski is known to play a role in neural tube (NT) development and muscle differentiation (Berk et al., 1997). Mice with targeted disruption of *c-Ski* on a mixed background display varied phenotypes (Colmenares et al., 2002). For the $Ski^{-/-}$ genotype on mixed backgrounds involving either 129P2 and C57BL/6J, or 129P2 and Swiss black, 80-88% of $Ski^{-/-}$ mice exhibit complex phenotypes, including a cranial NT defect resulting in exencephaly (Colmenares et al., 2002). The residual 12-15% of $Ski^{-/-}$ mice display midline facial clefting, suggesting that the phenotype of the null mutation is dependent on the genetic background.

Repeated backcrossing *Ski* heterozygotes with wildtype C57BL/6J or 129P2 and 129P3 mice resulted in a progressive increase of one phenotype over the other. Thus, when *Ski* heterozygotes were backcrossed with C57BL/6J wildtype mice**,** a loss of the exencephalic phenotype, and a proportional gain in frequency of facial clefting correlated with progressive enrichment in the C57BL/6J genome content (Colmenares et al., 2002). Following six generations of backcrossing with C57BL/6J, 78% of $Ski^{-/-}$ mice exhibited facial clefting, 11% were exencephalic and 11% were without abnormalities. In contrast, 83% of $Ski^{-/-}$ mice on an almost homogeneous 129P3 background were exencephalic. These experimental findings strongly suggest that the nature of the craniofacial anomaly in $Ski^{-/-}$ mice is influenced by strain-specific modifier genes (Colmenares et al., 2002). Interestingly, strong support for such a speculation comes from a recent report that identified chordin as a modifier for the craniofacial anomalies of Tbx1 mutations (Choi and Klingensmith, 2009).

Several studies employed microarray analysis to identify potential modifier genes (Alcaraz et al., 2011; Bleich et al., 2010; Coppin et al., 2007; Astrof et al., 2007). In the current study, an oligonucleotide-based microarray was employed in order to identify prospective strain-specific modifier gene candidates (in 129P3 and C57BL/6J wildtype strains) contributing to background-specific craniofacial abnormalities in various knockout mouse models derived from those wildtype strains.

METHODS

Procurement of developing neural tubes

Mature male and female C57BL6J (B6) and 129P3 (129) mice (Harlan, Inc.; Indianapolis, IN, USA) were housed in a climate-controlled room at a temperature of 22°C with an alternating 12-h dark-light cycle and were provided access to food and water *ad libitum.*

Mature male and female mice were mated over a two-hour window, the presence of a vaginal plug was considered evidence of mating, and the time designated as E0.5. Developmental staging was conducted following the method of Theiler (Theiler 1989). All studies were reviewed and approved, prior to their conduct, by the University of Louisville Institutional Animal Care and Use Committee (IACUC). Pregnant females of either B6 or 129 backgrounds were euthanized on E8.5 by carbon dioxide asphyxiation, the gravid uteri were removed, and individual embryos were dissected from decidual tissue and placed into ice-cold phosphate-buffered saline (PBS). Developing neural tubes from the most rostral aspect of the forebrain to the caudal aspect of the hindbrain (above the otic vesicle) were excised from E8.5 embryos (selected based on 5-8 somites; at this stage, any appreciable embryo-to-embryo variation in the developing neural tubes was not observed) and placed into 100μl extraction buffer (PicoPure RNA isolation kit, Arcturus Engineering, Mountain View, CA) for extraction of total RNA. In addition, to ensure that it develops at the same rate, morphogenesis of the neural tube was compared between B6J and 129 embryos at E8.5 and E9.0. The developmental status of the neural tubes was examined in no less than 25 embryos on each of E8.5 and E9.0 for each of the two strains. Particular attention was focused on closure points 1, 2 and 3, as described by Copp (2005) (Figure 1).

RNA Extraction and Target Synthesis

Total RNAs from E8.5 neural tube (NT) lysates were isolated using the PicoPure RNA isolation kit (Arcturus) following the manufacturer's recommendations. Briefly, tissue lysates in extraction buffer were incubated for 30 min at 42°C. After incubation, lysates were centrifuged, samples washed, and total cellular RNA eluted from RNA spin columns in 10μl of elution buffer. For each strain of mice (B6 or 129), four independent pools of 7 to 8 staged embryos were used to procure developing NTs for preparation of four distinct RNA samples. Those four distinct RNA samples were processed to prepare four separate sets of target RNAs from NTs from each of the two mouse strains. The four biological replicate RNA samples, corresponding to *each* mouse strain were then applied to individual GeneChips (i.e. eight samples and eight GeneChips total).

Preparation of Antisense RNA, Synthesis of Biotin-Labeled cRNA and GeneChip Hybridization

From the extracted total RNA, antisense RNA (aRNA) was produced using the RiboAmp OA-Kit (Arcturus) following manufacturer's instructions. RNA amplification was achieved by one round of first strand cDNA synthesis, second strand cDNA synthesis and *in vitro* transcription followed by a second round of first strand cDNA synthesis and second strand cDNA synthesis. The resultant double stranded cDNA was transcribed *in vitro* using a cRNA Transcript Labeling Kit (GeneChip Expression 3′ Amplification IVT labeling kit, Affymetrix) according to the manufacturer's instructions using biotinylated CTP and UTP. Following a 16-hour incubation at 37°C, the resultant biotin-labeled cRNA was purified with the cRNA Clean-up module (Affymetrix) and eluted in 21 μl of RNase-free water. The concentration of biotin-labeled cRNA was determined by spectrophotometric UV absorbance at 260/280 nm. The quality of the resulting aRNA was assessed on an Agilent RNA chip with Agilent 2100 Bioanalyzer (Agilent Technologies, Palo Alto, CA). Fifteen μg of labeled cRNA was fragmented in 40 μl 1X fragmentation buffer (40 mM Tris-acetate pH 8.1, 100 mM K-acetate, 30 mM Mg-acetate) for 35 min at 94°C and assessed by agarose gel electrophoresis. Fragmented cRNA was brought to a total volume of 300 μl with 1X hybridization buffer (100 mM MES, 1 M NaCl, 20 mM EDTA, 0.01% Tween 20), 100 μg/ml herring sperm DNA, 500 μg/ml acetylated BSA, 50 pM biotinylated control oligonucleotide B2 and 1X eukaryotic hybridization controls (1.5 pM BioB, 5.0 pM BioC, 25 pM BioB and 100 pM cre; Affymetrix; Santa Clara, CA). Target cRNAs derived from NTs of E8.5 embryos on either a C57BL6J or 129P3 genetic background, were hybridized to

individual GeneChips from an identical lot of Affymetrix Murine Genome 430 2.0 GeneChip arrays (containing 45,000 probe sets) for 16 hours. GeneChip arrays were washed and stained using antibody-mediated signal amplification and the Affymetrix Fluidics Station's standard Eukaryotic GE Wash 5/ protocol. Fluorescence intensities were determined using an Affymetrix GeneChip® Scanner 3000 (Affymetrix).

Microarray Data Analysis and Presentation

Images from the scanned chips were processed using Affymetrix GCOS 1.2 software (Affymetrix). Sample loading and variations in staining were standardized by scaling the average of the fluorescence intensities of all genes on an array to constant target intensity (250) for all arrays used. For analysis of the two different, B6 and 129 NT samples**,** the GeneChip image of the B6 samples was normalized to the corresponding images of the 129 samples across all probe pair sets. The full dataset was obtained using Affymetrix GCOS 1.2 and contained expression levels in B6 or 129 NT tissue samples for the expression level of over 39,000 transcripts and variants from over 34,000 well characterized mouse genes. CEL files containing individual raw chip data (probe intensities) were imported into GeneSpring 7.2 program and pre-processed using Robust Multi-chip Average, with GC-content background correction (GC-RMA). These data were then further processed using the 'per gene normalization' step in which all the samples were normalized against the median of the control samples. To define a set of statistically significant, differentially expressed genes, a one-way ANOVA (parametric test, assuming equal variances) was applied with 'Benjamini and Hochberg False Discovery Rate' as the multiple testing correction (p-value cutoff: 0.05). This restriction tested each of the 39,000 genes and ESTs and generated a list of 163 genes with statistically significant expression values. A filter on fold change (probes with fold differences >1.5 were considered significant) was next applied to these 163 genes and a second gene list was generated based on strain type (B6 vs. 129). This list included 157 genes that demonstrated either >1.5-fold higher or lower expression in NT tissue derived from the E8.5, B6 embryos with respect to that derived from E8.5, 129 embryos (Tables 1 and 2). A second set of differentially expressed genes with comparatively lower statistically significant expression was generated (following the same procedure as described above) without applying any multiple testing corrections but with a p-value cutoff of 0.05. Such a treatment generated a list of 3,351 genes which on application of a filter on fold change, yielded a list of 1,530 genes whose expression levels were either >1.5-fold more or less in NT tissue derived from the E8.5, B6 embryos with respect to that derived from the E8.5, 129 embryos (Supplementary Table 1).

Hierarchical clustering analysis was performed (on 157 genes demonstrating either >1.5-fold higher or lower expression) using the GeneSpring v7.2 software (Silicon Genetics, Inc., Redwood city, CA) to generate dendogram (Supplementary Fig. 1) representing functional categories of genes based on their expression profiles. Heat maps or clustered image maps were generated by dividing each measurement by the 50.0th percentile of all measurements in that sample, then setting the average value of expression level for each gene across the samples to 1.0. The resulting normalized signal value was plotted for each sample (values below 0.01 were set to 0.01). The list and the order of various genes in which they appear in the heat map can be viewed in tabular form (Tables 1 and 2). Data mining tools from 2 different software programs: NetAffx Analysis Center (Affymetrix, Santa Clara, CA), and GeneSpring v7.2 (Silicon Genetics, Inc., Redwood city, CA) were used.

Quantitative RT-PCR

cDNA was synthesized from amplified aRNA prepared from E8.5 B6 and 129 neural tubes using random hexamer primers and Superscript II reverse transcriptase (Invitrogen Life Technologies, Inc., Carlsbad, CA). Quantitative real-time PCR analysis was performed on a

TaqMan™ ABI Prism 7000 Sequence Detector System (Applied Biosystems, Foster City, CA). "Assays on Demand" custom primers and their corresponding fluorescence probes were obtained from Applied Biosystems. In all cases, both forward and reverse primers were used at a concentration of 900 nM while the concentration of the probe was 250 nM. For the PCR reaction, 1 ng of cDNA template was incubated with 0.2 mM dATP, dCTP, and dGTP, 0.4 mM dUTP, and 0.625 units of AmpliTaq Gold™ (Applied Biosystems, UK) in a final volume of 25 μl. Cycling parameters were as follows: 50°C for 2 min for probe and primer activation, 95°C for 10 min for DNA strand denaturation, followed by 40 cycles of denaturation at 95°C for 15 s, and primer extension at 60°C for 1 min. Furthermore, for each reaction, a parallel reaction lacking template was performed as a negative control. Raw data were acquired and processed with ABI Sequence Detector System software, version 1.0 (Applied Biosystems, UK). Results are represented as C_t values representing the number of cycles during the exponential phase of amplification necessary to reach a predetermined threshold level of PCR product as measured by fluorescence. Each cDNA sample was tested in duplicate and mean C_t values are reported. mRNA amounts for each gene were normalized to GAPDH mRNA present in each sample. Analysis was performed on 2-3 independent sets of cDNA and each cDNA sample was tested in duplicate. Statistical significance was determined by one-way ANOVA followed by Bonferroni's Multiple Comparison Test, using GraphPad Prism, v. 4.02 (GraphPad Software, Inc., San Diego, CA). P-values of <0.05 were considered significant.

Bioinformatic analysis of metabolic pathways in the developing neural tubes of B6 and 129 embryos

For investigation and comparison of different metabolic and/or canonical pathways and molecular interaction networks within the developing neural tubes from the two murine strains, the differentially expressed genes from B6 and 129 mouse strains were analyzed using the Ingenuity Systems Pathway Analysis (IPA) program (Ingenuity Systems, Mountain View, CA; http://www.ingenuity.com). In brief, a list of 1,530 gene transcripts (Supplementary Table 1) with significantly altered expression ($p<0.05$) within NTs from either 129 or B6 mouse strains was uploaded into Ingenuity database to obtain canonical/metabolic pathways that are more likely to be prevalent in one mouse strain versus the other. Enriched pathways comprising genes exhibiting increased expression in the developing neural tubes from the two strains are presented in supplementary tables 2 and 3. Although following Ingenuity analysis, many of these pathways appeared enriched but with apparently nonsignificant p-values, it is very important to note (as also emphasized by the IPA database) that there are numerous instances in biology where a biologically relevant phenomena might not be statistically significant and vice versa. This is especially true for signal transduction pathways, where the contribution of only one molecule within a specific canonical cascade could have critical biological impact.

RESULTS

Comparison of the rate of neural tube development between B6J and 129 embryos, focusing on closure points 1, 2 and 3 (Copp, 2005), revealed that closure (fusion) of the neural folds occurs at the same pace in both strains – confirming the notion that the NT develops at the same temporal rate in the two strains (Figure 1). A high-density oligonucleotide-based microarrays were utilized to analyze and compare gene expression profiles of isolated developing neural tubes (NTs) from E8.5, wildtype murine embryos on C57BL6J (B6) and 129P3 (129) backgrounds. Double-stranded cDNA mixtures derived from four independent sets of developing NT tissue samples from B6 and 129, E8.5 embryos (eight total samples) were transcribed into biotin-labeled cRNA which was used to probe separate Affymetrix high density GeneChip arrays containing oligonucleotide probes representing over 39,000

mouse genes and ESTs. When hybridized with cRNA derived from developing NTs from B6 and 129 embryos, 163 genes and ESTs demonstrated a detectable and statistically significant level of expression. Steady-state levels of 89 genes (probe sets) demonstrated a significantly higher level of expression (Table 1), and those of 68 genes (probe sets) demonstrated a significantly lower level of expression in the developing NT from E8.5, B6 embryos when compared to expression levels in NTs derived from E8.5, 129 embryos (Table 2). Such alterations in gene expression were reproducible in quadruplet samples of developing NTs. Graphical, two-dimensional, colorized representation of expression data as a heat map, and illustration of the arrangement of expression clusters in the form of a dendogram (Supplementary Fig. 1) were generated by hierarchical clustering analysis using the GeneSpring v7.2 software (Silicon Genetics, Redwood City, CA.). Genes were clustered into a number of functional categories including extracellular matrix and matrix associated proteins, growth and differentiation factors, miscellaneous signaling molecules, and transcription factors and DNA binding proteins.

Differential expression of many genes encoding multiple protein kinases and phosphatases, ECM proteins, structural proteins, proteases and adhesion molecules, transport proteins, proteins involved in ribosome biogenesis, apoptosis, and the immune response, were identified in developing NTs from both B6 and 129 embryos (Tables 1 and 2). In addition to the numerous genes belonging to the functional categories noted above, several ESTs as well as genes with a wide variety of physiological functions were identified in the developing NT (Tables 1 and 2). A substantial number of genes identified in the present microarray study, have been reported to be involved in mammalian NT development. Different expression levels of some of these genes in the developing NT of embryos from the two strains of mice might play a defining role in determining the observed strain-specific phenotypes of the S*ki* knockout mice. Examples of some “modifier’ candidate genes – known to be involved in neural tube development (Yoshida et al., 2004; Noce et al., 1993; Loebel et al., 2004; Heil et al., 2001; Kuan et al., 1999; Kester et al., 2000) – differentially expressed in the developing NTs of B6 vs 129 mice are: *Phgdh, NT fin12, Shmt, Mapk8* (JNK1) and *Tsc22d1* (TSC22 domain family, member 1).

Using TaqMan quantitative real-time PCR (Bustin et al., 2000), gene expression profiling results obtained by microarray analyses were independently validated. Relative expression levels of twelve candidate genes demonstrating diverse levels of expression in the developing NT derived from E8.5, B6 and 129 embryos, were quantified and compared to the corresponding expression levels determined by the microarray technique. Expression profiles of eleven out of the twelve mRNAs tested were found to be in consistent agreement when comparing the two methods (Table 3).

Following analysis with Ingenuity, pathways, comprising genes exhibiting increased expression in the developing NTs from either B6 or 129 strains, and with differential enrichment between the two strains, are listed in supplementary tables 2 and 3. Pathways more enriched in the developing NT from B6 embryos, when compared to NTs from 129 embryos, include C21 steroid hormone metabolism, Ephrin receptor signaling, Inositol phosphate metabolism/signaling, Integrin signaling, and phenylalanine metabolism, among others (Supplementary Table 2). Pathways more enriched in 129 NTs include Wnt/β;-catenin signaling, valine, leucine and isoleucine metabolism, pyrimidine metabolism and BMP signaling, among others (Supplementary Table 3). Various differentially expressed genes participating in and/or associated with each enriched pathway are also listed in supplementary tables 2 and 3.

DISCUSSION

In order to analyze gene function during embryogenesis, use of genetically engineered mice in which one or more genes have been turned off via gene targeting has proved to be extraordinarily revealing. Additionally, targeting of numerous loci has resulted in disparate phenotypes depending on the genetic background of the targeted mouse strains (Matsuo et al., 1995; Proetzel et al., 1995; Rozmahel et al., 1996; LeCouter et al., 1998; Wojnowski et al., 1998; Wawersik et al., 1999). Phenotypic alterations seen in null-mutants from two different strains of mice may be attributable to dissimilarities in the genetic background (such as presence of strain-specific modifier genes) of the two inbred strains (Gerlai, 1996). Genetic analysis suggests that the facial clefting exhibited by *Ski*$^{-/-}$ mice on a C57BL6J (B6) background, and the exencephaly seen in *Ski*$^{-/-}$ mice on a 129P3 (129) background are governed, in part, by combinations of strain-specific modifier genes (Colmenares et al., 2002).

While recognized that genetic backgrounds can significantly influence phenotypes associated with gene-targeted mice, the impact on mRNA expression profiles is inadequately appreciated (Gerlai, 1996; Suzuki and Nakayama, 2003). Genomic array technology has been increasingly utilized to identify individual genes and signaling pathways critical for embryonic development (for reviews see, Ko, 2006; Hamatani et al., 2006) as well as differentially expressed genes in mice with different genetic backgrounds (Jelcick et al., 2011; Alcaraz et al., 2011; Bleich et al., 2010; Coppin et al., 2007; Astrof et al., 2007).

While strain-specific modifier genes have been hypothesized as causal in regulating expression of craniofacial phenotypes in *Ski*$^{-/-}$ mice on B6 and 129 genetic backgrounds (Colmenares et al., 2002), the current study attempts to identify some of these “modifiers.” The formation of the cranial neural tube (NT) necessitates coordinated morphogenetic shaping, bending and closure of the neural plate (Sakai 1989) as well as stage-specific cellular proliferation and neuroepithelial apoptosis (McKay et al., 1994). Thus, “modifier’ candidate genes are likely to be among those that are differentially expressed in the NTs of B6 vs 129 mice during the stage when these processes are occurring.

Post-translational modification of proteins via enzymatic phosphorylation by protein kinases and dephosphorylation by protein phosphatases is well documented as one of the most important means by which cellular signals can be transduced into multiple biological effects. Highlighting the significance of such modifications during development of the NT, expression of genes encoding multiple protein kinases and phosphatases were identified in developing NTs from both B6 and 129 embryos. Moreover, during development, the extracellular matrix (ECM), provides support and anchorage for cells, and regulates intercellular communication. The ECM sequesters a wide range of cellular growth factors, and their release allows rapid and local growth factor-mediated activation of cellular functions, without de novo synthesis. Supporting the notion that synthesis/turnover of the ECM contributes to NT development, expression of a number of genes encoding multiple ECM proteins, structural proteins, proteases and adhesion molecules were detected in NTs derived from E8.5, B6 and 129 embryos..

In addition, the expression of several candidate genes likely to function as potential “modifiers”, differentially expressed in the developing NTs of B6 vs. 129 mice, and reported to be involved in mammalian NT development such as *Phgdh, NT fin12, SHMT, Mapk8* (JNK1) and *Tsc22d1* (TSC22 domain family, member 1) (Yoshida et al., 2004; Noce et al., 1993; Loebel et al., 2004; Heil et al., 2001; Kuan et al., 1999; Kester et al., 2000), were also documented. However, it should be noted here that although the Affymetrix arrays provide

significant coverage of the transcribed mouse genome on a single array (e.g. 45,000 probe sets analyze the expression level of over 39,000 transcripts and variants from over 34,000 well characterized mouse genes), searching for modifiers with this microarray approach might be limited in scope as not all modifiers are expected to show differential gene expression between strains. *Phgdh* encodes for D-3-Phosphoglycerate dehydrogenase (Phgdh)**,** an enzyme essential for *de novo* L-serine biosynthesis via a phosphorylated pathway vital for brain development during embryogenesis (Shimizu et al., 2004). Expressed exclusively by neuroepithelium and radial glia in the developing brain, disruption of the murine *Phgdh* gene results in embryonic lethality, accompanied by severe neurodevelopmental defects (Yoshida et al., 2004) including hypoplasia of the telencephalon, diencephalon, and mesencephalon (Shimizu et al., 2004). In the present study, two ESTs with strong similarity to the gene encoding murine *Phgdh***,** demonstrated high levels of expression in NTs isolated from E8.5, B6 embryos in comparison to those from E8.5, 129 embryos (Table 1). This result was verified by QRT-PCR (Table 3). In view of the aforementioned findings, it might be argued that significantly elevated expression of *Phgdh* in the neuroepithelium of B6 embryo is functioning as a modifier of the exencephalic phenotype of these embryos lacking genes (e.g. *Ski*$^{--}$) indispensible for NT development. In contrast, reduced level of expression of Phgdh in the neuroepithelium of 129 embryos fails to modify exencephaly resulting from such deletion.

NT fin12, a gene encoding a novel zinc finger protein, belonging to the C2H2-Kruppel-type gene family is expressed during embryogenesis. NT fin12 transcripts have been revealed by *in situ* hybridization in the neuroectoderm of embryos on E8.5-13.5, as well as in peripheral ganglia derived from neural crest cells**,** neural placodes and in motor nerve cells in the central nervous system (Noce et al., 1993). The current comparative microarray analysis demonstrated a 14.5-fold higher level of expression of an EST similar to the gene encoding *NT fin12* in E8.5, B6 NTs, in comparison to E8.5, 129 NTs (Table 1). This result was verified by QRT-PCR (Table 3). Based on the spatiotemporal expression of *NT fin12* during NT development**,** and the elevated expression in NTs from B6 embryos, this gene can be considered to be a candidate modifier of the exencephalic phenotype in B6 embryos.

The enzyme serine hydroxymethyltransferase (Shmt) catalyzes the reversible conversion of serine and tetrahydrofolate (THF) to glycine and 5,10-methylene THF. It has been argued that due to the involvement of Shmt in cellular folate/homocysteine metabolism, polymorphisms in the gene encoding this enzyme might result in elevated homocysteine levels and hence, disturbed folate-dependent homocysteine metabolism leading to a NT defect (Heil et al., 2001). A very recent study by Beaudin et al. (2011) documented exencephaly in *Shmt1*$^{+/-}$ and *Shmt1*$^{-/-}$ embryos. The gene encoding Shmt is repressed by retinoic acid (RA) (Nakshatri et al., 1996). These same authors suggest that since Shmt activity is elevated during the synthetic phase of the cell cycle, repression of *Shmt* expression may be a vital step in RA-induced cell growth arrest and differentiation. Moreover, since the Ski oncoprotein can repress RA receptor signaling (Dahl et al 1998) derepressed RA signaling in *Ski*-null embryos may be responsible for enhanced suppression of Shmt1 activity in the developing NT. We have shown a significantly higher level (>3.5-fold) of expression of the S*hmt1* gene in E8.5, B6 NTs when compared to the 129 NTs (Table 1). Thus, S*hmt1* may act as a modifier of the exencephalic phenotype in the B6 embryo by maintaining the balance between cell proliferation and apoptosis within the neural folds.

The three candidate modifier genes discussed above are expressed at significantly higher levels in NTs derived from E8.5, B6 embryos when compared to their expression in the NTs of E8.5, 129 embryos. In the following section, we discuss another set of candidate genes,

these demonstrating significantly increased expressions in E8.5 NTs from 129 embryos when compared to their expressions in the NTs of B6 embryos.

c-Jun N-terminal protein kinases (JNKs), or stress-activated protein kinases (SAPKs) (Hibi et al., 1993), represent a subfamily of the mitogen-activated protein kinase (MAPK) superfamily. There are two ubiquitously expressed isoforms of JNK (JNK1 and JNK2), as well as a tissue-specific isoform, JNK3 (Chang and Karin, 2001, Davis 2000, Lin 2003). JNKs play vital roles in regulating a range of cellular activities including gene expression, cell survival and apoptosis (Chang and Karin, 2001, Davis 2000, Lin 2003). The character of these actions is cell-type specific and dependent on the activity of other signaling pathways (Lin 2003, Liu et al., 2004). Both JNK1 and JNK2 have been implicated in survival of neuronal cells during murine brain development (Kuan et al., 1999; Sabapathy et al., 1999). Moreover, *Jnk1/Jnk2* double null mutant mice exhibit severe spatial dysregulation of neural apoptosis during early brain development and exencephaly (Kuan et al., 1999). Indeed, JNK1 and JNK2 are capable of displaying both pro- and anti-apoptotic functions during neurogenesis (Lin 2003, Kuan et al 1999). Our data revealed a significantly elevated level of expression (57.5-fold) of the gene encoding MAPK8 or JNK1 in the E8.5, 129 NT when compared to their expression in the NTs of B6 embryos (Table 2). These data collectively suggest that MAPK8**,** or JNK1-encoding gene**,** may be modifying the orofacial clefting phenotype in the NTs of these mice by inhibiting apoptosis in the forebrain region (e.g. in the absence of c-Ski). In contrast, the pro-apoptotic activity of this kinase in the highly apoptotic *Ski*$^{-/-}$ midbrain-hindbrain region (Colmenares et al., 1997) may be contributing toward the exencephalic phenotype in the 129 *Ski* knockout embryos.

TGFß stimulated clone-22 (TSC-22), a downstream target of TGFß signaling, represents an 18-kD leucine zipper containing transcription factor that lacks a basic DNA binding motif (Kester et al., 1999). TGFß signaling can be stimulated by TSC-22 via its association with**,** and modulation of**,** the transcriptional activities of Smad3 and Smad4 (Choi et al., 2005). Indeed, TSC-22 mediates TGFß-induced apoptosis in human gastric carcinoma cells (Ohta et al., 1997). TSC-22 demonstrated robust expression in the primitive heart, intermediate mesoderm and NT of the E8.5 murine embryo (Kester et al., 2000). We have shown increased (18.2-fold) expression of the gene encoding TSC-22 in NTs from E8.5, 129 embryos when compared to expression in NTs from E8.5, B6 embryos (Table 2). In view of the pro-apoptotic function of TSC-22**,** and its significantly elevated expression in the developing NTs of 129 embryos**,** the data support the hypothesis that TSC-22 may be one of several genes contributing to the exencephalic phenotype in 129 embryos.

The ultimate objective of this study is to speculate modifier(s) affecting failure of fusion of the developing neural tube at the two different closure regions (site 2 vs. 3; Figure 1) in *Ski*$^{-/-}$ embryos; apparently, the underlying mechanism is not that exencephaly happens, but more than orofacial clefting shifts to exencephaly. Furthermore, modification of the phenotypic outcome within the two murine strains could be due to dysregulation of spatiotemporal gene expression (during the critical period of NT development) governed by particular strain-specific modifier gene(s). It is also possible that strain-specific modifier gene(s) is directing expression of one or more homeotic genes (governing the fusion of the neural folds) rather differently in the 129 P3 and B6J, embryos, resulting in dissimilar phenotypic outcomes.

Our data allow identification of several strain-specific candidate modifiers of craniofacial development in knockout mouse models derived from 129 P3 and B6J *background strains*. The gene expression database generated from our study should be of value when compared to other gene expression databases from nonisogenic littermates.

Pathway analysis of differentially expressed genes

Ingenuity pathway analysis program (IPA; Ingenuity Systems, Redwood City, CA), and two other online databases (NIH-DAVID**,** KEGG pathway database), were used to identify differentially enriched metabolic pathways**,** molecular interaction and reaction networks in B6 vs 129 NTs. A number of interesting differentially enriched pathways were identified.

Steroid hormones perform a key role in neural development and the effects of some of these hormones e.g. androgens, estrogens, glucocorticoids and progesterone, on the developing brain are well established (Quadros et al., 2007; Jelks et al., 2007). Moreover, an association between development of NT defects and corticosteroids has been reported (Hendrickx and Tarara, 1990; Dindar et al., 1999; Trollmen et al., 2001). Ingenuity pathway analysis revealed that C21 steroid hormone metabolism is the most enriched pathway in genes demonstrating enhanced expression in B6 NT, but is not enriched in those displaying increased expression in 129 NTs (Supplementary Tables 2 and 3). Likewise, androgen and estrogen metabolism is enriched only in 129 NT (Supplementary Tables 2 and 3). In consideration of the above findings, it can be argued that comparatively higher metabolic activities (as a result of greater enrichment) of the C21 steroid hormone metabolism as well as the androgen and estrogen metabolism pathways, might serve as a protective measure towards emergence of the exencephalic phenotype in B6 embryos in the absence of genes (e.g *Ski*$^{-/-}$) indispensible for NT development. Higher cholesterol levels during pregnancy have been linked to higher incidence of NT defects. Since C21 steroid hormone metabolism pathway and the androgen and estrogen metabolism pathway both utilizes cholesterol, higher activities of these two pathways in B6J NT may result in comparatively lower levels of cholesterol and hence contribute to a lower incidence of exencephaly in B6J NT.

Complex interplay between BMP/TGFß, Wnt, FGF and hedgehog signaling cascades is known to contribute to induction of the neural plate and patterning of neural and non-neural ectoderm (Altmann and Brivanlou, 2001; Bally-Cuif and Hammerschmidt, 2003). These morphogens provide signals permissive to the progression and maintenance of growth control in the developing neural tube (Cayuso and Marti, 2005). Several studies implicated altered Wnt signaling to generation of neural tube defects in developing embryos and the significance of BMP signaling in neural tube morphogenesis (Shariatmadari et al., 2005; Anderson et al., 2006; Ybot-Gonzalez et al., 2007; Pavlinkova et al., 2008). Interestingly, pathway analysis with the Ingenuity program (involving higher numbers (1530 as opposed to 157 used previously) of differentially expressed genes), revealed that the Wnt signaling cascade is the most enriched canonical pathway, and also, that this pathway is not enriched in genes displaying enhanced expression in the 129 NT (Supplementary Tables 2 and 3). BMP signaling has also emerged as biologically interesting among genes demonstrating enhanced expression in the neural tube from 129 embryos (Supplementary Table 3). Thus, one may speculate that higher activities of the Wnt and BMP signaling pathways (because of enrichment) in 129 NT may offer protection against the orofacial clefting but may be two of several contributing factors towards generation of the exencephalic phenotype in knockout models (e.g. *Ski*$^{-/-}$) derived from the 129 strains.

Neurulation relies on cellular adhesion, a crucial physical property of the cells and tissues both inside and outside the neural plate. A number of studies highlighted direct involvement of cell adhesion molecules in cranial neurulation demonstrating the occurrence of neural tube defects in mice lacking Ephrins or Integrins (Holmberg et al., 2000; Colas and Schoenwolf, 2003; Altick et al., 2005). Exencephaly was reported in mice deficient in EphrinB5 as well as in EphrinB2:EphrinB3 compound mutant mice (Holmberg et al., 2000; Altick et al., 2005). Emigration of neural crest cells, a prerequisite for neural tube fusion, was shown to be inhibited (leading to Neural tube defects) by antisense oligonucleotides to various integrins (Kil et al., 1996) and anomalous neurulation was also observed in embryos

lacking Integrin α6 (Lallier et al., 1996; Colas and Schoenwolf, 2003). All these findings reinforce the indispensability of Ephrin and Integrin signaling in neural tube morphogenesis. Interestingly, in the present study, Ingenuity pathway analysis revealed both Ephrin and Integrin signaling as biologically meaningful consisting of genes exhibiting enhanced expression in the developing neural tubes from B6J embryos (Supplementary Tables 2 and 3). In view of these experimental evidences it can be argued that apparent lower activities of Ephrin and Integrin signaling in 129 neural tubes might render this strain of embryos more susceptible to exencephaly (than B6J embryos) when they are devoid of genes crucial for neural tube development such as the transcriptional repressor, Ski.

Numerous studies documented the centrality of Inositol Phosphate (IP) metabolism/signaling in embryogenesis (for a review, see Seeds et al., 2007). Indispensability of IP signaling in neural tube morphogenesis is highlighted by the incidence of exencephaly in embryos lacking several members of this metabolic/signaling pathway. For example, exencephaly was reported in mice deficient in ITPK1 (Inositol 1,3,4-trisphosphate 5/6-kinase), Ipk2 (inositol polyphosphate multikinase) and PIP2 (phospholipid phosphatidylinositol 4, 5-bisphosphate) (Frederick et al., 2005; Wang et al., 2007; Wilson et al., 2009). Analysis with the Ingenuity pathway program revealed the importance of Inositol Phosphate metabolism/signaling within genes demonstrating augmented expression in B6J neural tube (Supplementary Tables 2 and 3). Consequently, comparative lower activity of Inositol Phosphate (IP) metabolism/signaling pathway might render the 129 embryos prone to exencephaly as opposed to their B6J counterparts.

Microarray technology is one of several present-day molecular genetic applications that enable researchers to generate a gene expression “fingerprint” of thousands of genes in a single experiment. In the present study, an oligonucleotide-based microarray approach has been utilized to create a comparative “molecular fingerprint” representing gene expression at a critical stage of neural tube development in two different in-bred stains of mouse. The principal objective of this endeavor was to ascertain potential strain-specific modifier genes and biological pathways contributing towards background-specific craniofacial anomalies in various knockout mouse models. Results of the current study should provide investigators with useful gene expression data on neural tube development obtained from the analysis of embryos from two inbred strains, 129P3 and C57BL/6, that are standard murine strains used in gene-targeting research.

Supplementary Material

Refer to Web version on PubMed Central for supplementary material.

Acknowledgments

This research was supported in part by NIH grants HD053509 and DE018215 to RMG; AA13205 to MMP; a grant from the Cleft Palate Foundation to PM; The Commonwealth of Kentucky Research Challenge Trust Fund; and P20 RR017702 from the COBRE program of the National Center for Research Resources to RMG.

REFERENCES

Alcaraz WA, Chen E, Valdes P, Kim E, Lo YH, Vo J, Hamilton BA. Modifier genes and non-genetic factors reshape anatomical deficits in Zfp423-deficient mice. Hum Mol Genet. 2011; 20:3822–3830. [PubMed: 21729880]

Altick AL, Dravis C, Bowdler T, Henkemeyer M, Mastick GS. EphB receptor tyrosine kinases control morphological development of the ventral midbrain. Mech Dev. 2005; 122:501–512. [PubMed: 15804564]

Altmann CR, Brivanlou AH. Neural patterning in the vertebrate embryo. Int Rev Cytol. 2001; 203:447–482. [PubMed: 11131523]

Anderson RM, Stottmann RW, Choi M, et al. Endogenous bone morphogenetic protein antagonists regulate mammalian neural crest generation and survival. Dev Dyn. 2006; 235:2507–2520. [PubMed: 16894609]

Astrof S, Kirby A, Lindblad-Toh K, Daly M, Hynes RO. Heart development in fibronectin-null mice is governed by a genetic modifier on chromosome four. Mech Dev. 2007; 124:551–558. [PubMed: 17628448]

Aziz RK, Kansal R, Abdeltawab NF, Rowe SL, Su Y, et al. Susceptibility to severe Streptococcal sepsis: use of a large set of isogenic mouse lines to study genetic and environmental factors. Genes Immun. 2007; 8:404–415. [PubMed: 17525705]

Bally-Cuif L, Hammerschmidt M. Induction and patterning of neuronal development, and its connection to cell cycle control. Curr Opin Neurobiol. 2003; 13:16–25. [PubMed: 12593978]

Baust C, Baillie GJ, Mager DL. Insertional polymorphisms of ETn retrotransposons include a disruption of the wiz gene in C57BL/6 mice. Mamm Genome. 2002; 13:423–428. [PubMed: 12226707]

Berk M, Desai SY, Heyman HC, et al. Mice lacking the ski proto-oncogene have defects in neurulation, craniofacial, patterning, and skeletal muscle development. Genes Dev. 1997; 11:2029–2039. [PubMed: 9284043]

Bleich A, Büchler G, Beckwith J, Petell LM, Affourtit JP, et al. Cdcs1 a major colitis susceptibility locus in mice; subcongenic analysis reveals genetic complexity. Inflamm Bowel Dis. 2010; 16:765–775. [PubMed: 19856416]

Boross P, Arandhara VL, Martin-Ramirez J, Santiago-Raber ML, Carlucci F, et al. The inhibiting Fc receptor for IgG, FcγRIIB, is a modifier of autoimmune susceptibility. J Immunol. 2011; 187:1304–1313. [PubMed: 21724994]

Bronner-Fraser M. An antibody to a receptor for fibronectin and laminin perturbs cranial neural crest development in vivo. Dev Biol. 1986; 117:528–536. [PubMed: 2944780]

Bustin SA. Absolute quantification of mRNA using real-time reverse transcription polymerase chain reaction assays. J Mol Endocrinol. 2000; 25:169–193. [PubMed: 11013345]

Cayuso J, Marti E. Morphogens in motion: growth control of the neural tube. J Neurobiol. 2005; 64:376–387. [PubMed: 16041754]

Chang L, Karin M. Mammalian MAP kinase signaling cascades. Nature. 2001; 410:37–40. [PubMed: 11242034]

Choi SJ, Moon JH, Ahn YW, et al. Tsc-22 enhances TGF-beta signaling by associating with Smad4 and induces erythroid cell differentiation. Mol Cell Biochem. 2005; 271:23–28. [PubMed: 15881652]

Choi M, Klingensmith J. Chordin is a modifier of tbx1 for the craniofacial malformations of 22q11 deletion syndrome phenotypes in mouse. PLoS Genet. 2009; 5:e1000395. [PubMed: 19247433]

Colas JF, Schoenwolf GC. Differential expression of two cell adhesion molecules, Ephrin-A5 and Integrin alpha6, during cranial neurulation in the chick embryo. Dev Neurosci. 2003; 25:357–365. [PubMed: 14614263]

Colmenares C, Heilstedt HA, Shaffer LG, et al. Loss of the SKI proto-oncogene in individuals affected with 1p36 deletion syndrome is predicted by strain-dependent defects in Ski−/− mice. Nat Genet. 2002; 30:106–109. [PubMed: 11731796]

Copp AJ. Neurulation in the cranial region – normal and abnormal. J Anat. 2005; 207:623–635. [PubMed: 16313396]

Coppin H, Darnaud V, Kautz L, Meynard D, Aubry M, et al. Gene expression profiling of Hfe−/− liver and duodenum in mouse strains with differing susceptibilities to iron loading: identification of transcriptional regulatory targets of Hfe and potential hemochromatosis modifiers. Genome Biol. 2007; 8:R221. [PubMed: 17945001]

Dahl R, Kieslinger M, Beug H, et al. Transformation of hematopoietic cells by the Ski oncoprotein involves repression of retinoic acid receptor signaling. Proc Natl Acad Sci USA. 1998; 95:11187–11192. [PubMed: 9736711]

Davis RJ. Signal transduction by the JNK group of MAP kinases. Cell. 2000; 103:239–252. [PubMed: 11057897]

de Mooij-van Malsen JG, Yu KL, Veldman H, Oppelaar H, van den Berg LH, et al. Variations in ventral root axon morphology and locomotor behavior components across different inbred strains of mice. Neuroscience. 2009; 164:1477–1483. [PubMed: 19778584]

Deak KL, Boyles AL, Etchevers HC, et al. SNPs in the neural cell adhesion molecule 1 gene (NCAM1) may be associated with human neural tube defects. Hum Genet. 2005; 117:133–142. [PubMed: 15883837]

Dindar H, Kanmaz T, Cakmak M, et al. The split notochord syndrome with dorsal enteric fistula, meningomyelocele and imperforate anus. Turk J Pediatr. 1999; 41:147–150. [PubMed: 10770692]

Donehower LA, Harvey M, Vogel H, et al. Effects of genetic background on tumorigenesis in p53-deficient mice. Mol Carcinog. 1995; 14:16–22. [PubMed: 7546219]

Errijgers V, Fransen E, D'Hooge R, De Deyn PP, Kooy RF. Effect of genetic background on acoustic startle response in fragile X knockout mice. Genet Res (Camb). 2008; 90:341–345. [PubMed: 18840308]

Ewart-Toland A, Mounzih K, Qiu J, et al. Effect of the genetic background on the reproduction of leptin-deficient obese mice. Endocrinology. 1999; 140:732–738. [PubMed: 9927300]

Finn R, Kovács AD, Pearce DA. Altered sensitivity to excitotoxic cell death and glutamate receptor expression between two commonly studied mouse strains. J Neurosci Res. 2010; 88:2648–2660. [PubMed: 20544821]

Frederick JP, Mattiske D, Wofford JA, Megosh LC, Drake LY, et al. An essential role for an inositol polyphosphate multikinase, Ipk2, in mouse embryogenesis and second messenger production. Proc Natl Acad Sci USA. 2005; 102:8454–8459. [PubMed: 15939867]

Gerlai R. Gene-targeting studies of mammalian behavior: is it the mutation or the background genotype? Trends Neurosci. 1996; 19:177–181. [PubMed: 8723200]

Hamatani T, Ko MSh, Yamada M, Kuji N, Mizusawa Y, et al. Global gene expression profiling of preimplantation embryos. Hum Cell. 2006; 19:98–117. [PubMed: 17204093]

Harvey M, McArthur MJ, Montgomery CA Jr, et al. Genetic background alters the spectrum of tumors that develop in p53-deficient mice. FASEB J. 1993; 7:938–943. [PubMed: 8344491]

Heil SG, Van der Put NM, et al. Is mutated serine hydroxymethyltransferase (SHMT) involved in the etiology of neural tube defects? Mol Genet Metab. 2001; 73:164–172. [PubMed: 11386852]

Hendrickx AG, Tarara RP. Triamcinolone acetonide-induced meningocele and meningoencephalocele in rhesus monkeys. Am J Pathol. 1990; 136:725–727. [PubMed: 2316629]

Hibi M, Lin A, Smeal T, et al. Identification of an oncoprotein- and UV-responsive protein kinase that binds and potentiates the c-Jun activation domain. Genes Dev. 1993; 7:2135–2148. [PubMed: 8224842]

Holmberg J, Clarke DL, Frisén J. Regulation of repulsion versus adhesion by different splice forms of an Eph receptor. Nature. 2000; 408:203–206. [PubMed: 11089974]

Jelcick AS, Yuan Y, Leehy BD, Cox LC, Silveira AC, et al. Genetic variations strongly influence phenotypic outcome in the mouse retina. PLoS One. 2011; 6:e21858. [PubMed: 21779340]

Jelks KB, Wylie R, Floyd CL, et al. Estradiol targets synaptic proteins to induce glutamatergic synapse formation in cultured hippocampal neurons: critical role of estrogen receptor-alpha. Neurosci. 2007; 27:6903–6913.

Kester HA, Blanchetot C, den Hertog J, et al. Transforming growth factor-beta-stimulated clone-22 is a member of a family of leucine zipper proteins that can homo- and heterodimerize and has transcriptional repressor activity. J Biol Chem. 1999; 274:27439–27447. [PubMed: 10488076]

Kester HA, Ward-van Oostwaard TM, Goumans MJ, et al. Expression of TGF-beta stimulated clone-22 (TSC-22) in mouse development and TGF-beta signaling. Dev Dyn. 2000; 218:563–572. [PubMed: 10906776]

Kil SH, Lallier T, Bronner-Fraser M. Inhibition of cranial neural crest adhesion in vitro and migration in vivo using integrin antisense oligonucleotides. Dev Biol. 1996; 179:91–101. [PubMed: 8873756]

Ko MS. Expression profiling of the mouse early embryo: reflections and perspectives. Dev Dyn. 2006; 235:2437–2448. [PubMed: 16739220]

Kobayashi S, Hirano T, Kakinuma M, et al. Transcriptional repression and differential splicing of Fas mRNA by early transposon (ETn) insertion in autoimmune lpr mice. Biochem Biophys Res Commun. 1993; 191:617–624. [PubMed: 7681668]

Kuan CY, Yang DD, Samanta Roy DR, et al. The Jnk1 and Jnk2 protein kinases are required for regional specific apoptosis during early brain development. Neuron. 1999; 22:667–676. [PubMed: 10230788]

Lallier TE, Whittaker CA, DeSimone DW. Integrin alpha 6 expression is required for early nervous system development in Xenopus laevis. Development. 1996; 122:2539–2554. [PubMed: 8756298]

LeCouter JE, Kablar B, Whyte PFM, et al. Strain-dependent embryonic lethality in mice lacking the retinoblastoma-related p130 gene. Development. 1998; 125:4669–4679. [PubMed: 9806916]

Lin A. Activation of the JNK signaling pathway: breaking the brake on apoptosis. Bioessays. 2003; 25:1–8. [PubMed: 12508274]

Linsenbardt DN, Moore EM, Gross CD, Goldfarb KJ, Blackman LC, et al. Sensitivity and tolerance to the hypnotic and ataxic effects of ethanol in adolescent and adult C57BL/6J and DBA/2J mice. Alcohol Clin Exp Res. 2009; 33:464–476. [PubMed: 19120054]

Liu J, Minemoto Y, Lin A. c-Jun N-terminal protein kinase 1 (JNK1), but not JNK2, is essential for tumor necrosis factor alpha-induced c-Jun kinase activation and apoptosis. Mol Cell Biol. 2004; 24:10844–10856. [PubMed: 15572687]

Loebel DA, Tsoi B, Wong N, et al. Restricted expression of ETn-related sequences during post-implantation mouse development. Gene Exp Patterns. 2004; 4:467–471.

Lu SY, Jin Y, Li X, Sheppard P, Bock ME, et al. Embryonic survival and severity of cardiac and craniofacial defects are affected by genetic background in fibroblast growth factor-16 null mice. DNA Cell Biol. 2010; 29:407–415. [PubMed: 20618076]

Mager DL, Freeman JD. Novel mouse type D endogenous proviruses and ETn elements share long terminal repeat and internal sequences. J Virol. 2000; 74:7221–7229. [PubMed: 10906176]

Matsuo I, Kuratani S, Kimura C, et al. Mouse Otx2 functions in the formation and patterning of rostral head. Genes Dev. 1995; 9:2646–2658. [PubMed: 7590242]

McKay IJ, Muchamore I, Krumlauf R, et al. The kreisler mouse: a hindbrain segmentation mutant that lacks two rhombomeres. Development. 1994; 120:2199–2211. [PubMed: 7925021]

Nakshatri H, Bouillet P, Bhat-Nakshatri P, et al. Isolation of retinoic acid-repressed genes from P19 embryonal carcinoma cells. Gene. 1996; 174:79–84. [PubMed: 8863732]

Newgreen DF, Kerr RS, Minichiello J, et al. Changes in cell adhesion and extracellular matrix molecules in spontaneous spinal neural tube defects in avian embryos. Teratology. 1997; 55:195–207. [PubMed: 9181673]

Noce T, Fujiwara Y, Ito M, et al. A novel murine zinc finger gene mapped within the tw18 deletion region expresses in germ cells and embryonic nervous system. Dev Biol. 1993; 155:409–422. [PubMed: 8432396]

Ohta S, Yanagihara K, Nagata K. Mechanism of apoptotic cell death of human gastric carcinoma cells mediated by transforming growth factor beta. Biochem J. 1997; 324:777–782. [PubMed: 9210400]

Painsipp E, Köfer MJ, Sinner F, Holzer P. Prolonged depression-like behavior caused by immune challenge: influence of mouse strain and social environment. PLoS One. 2011; 6:e20719. [PubMed: 21673960]

Pavlinkova G, Salbaum JM, Kappen C. Wnt signaling in caudal dysgenesis and diabetic embryopathy. Birth Defects Res A Clin Mol Teratol. 2008; 82:710–719. [PubMed: 18937363]

Proetzel G, Pawlowski SA, Wiles MV, et al. Transforming growth factor-b3 is required for secondary palate fusion. Nat Genet. 1995; 11:409–414. [PubMed: 7493021]

Quadros PS, Pfau JL, Wagner CK. Distribution of progesterone receptor immunoreactivity in the fetal and neonatal rat forebrain. J Comp Neurol. 2007; 504:42–56. [PubMed: 17614295]

Rozmahel R, Wilschanski M, Matin A, et al. Modulation of disease severity in cystic fibrosis transmembrane conductance regulator deficient mice by a secondary genetic factor. Nat Genet. 1996; 12:280–287. [PubMed: 8589719]

Sabapathy K, Jochum W, Hochedlinger K, et al. Defective neural tube morphogenesis and altered apoptosis in the absence of both JNK1 and JNK2. Mech Dev. 1999; 89:115–124. [PubMed: 10559486]

Sakai Y. Neurulation in the mouse: manner and timing of neural tube closure. Anat Rec. 1989; 223:194–203. [PubMed: 2712345]

Sanford LP, Kallapur S, Ormsby I, et al. Influence of genetic background on knockout mouse phenotypes. Methods Mol Biol. 2001; 158:217–225. [PubMed: 11236659]

Seeds AM, Frederick JP, Tsui MM, York JD. Roles for inositol polyphosphate kinases in the regulation of nuclear processes and developmental biology. Adv Enzyme Regul. 2007; 47:10–25. [PubMed: 17467778]

Shah AP, Siedlecka U, Gandhi A, Navaratnarajah M, Al-Saud SA, et al. Genetic background affects function and intracellular calcium regulation of mouse hearts. Cardiovasc Res. 2010; 87:683–693. [PubMed: 20413651]

Shariatmadari M, Peyronnet J, Papachristou P, et al. Increased Wnt levels in the neural tube impair the function of adherens junctions during neurulation. Mol Cell Neurosci. 2005; 30:437–451. [PubMed: 16154760]

Shimizu M, Furuya S, Shinoda Y, et al. Functional analysis of mouse 3-phosphoglycerate dehydrogenase (Phgdh) gene promoter in developing brain. J Neurosci Res. 2004; 76:623–632. [PubMed: 15139021]

Suzuki Y, Nakayama M. Differential Profiles of Genes Expressed in Neonatal Brain of 129X1/SvJ and C57BL/6J Mice: A database to aid in analyzing DNA microarrays using nonisogenic gene-targeted mice. DNA Res. 2003; 10:263–275. [PubMed: 15029957]

Theiler, K. Springer-Verlag; 1989. The House Mouse.

Trollmann R, Langhans B, Strehl E, et al. A cross-sectional study of dehydroepiandrosterone sulfate in prepubertal children with myelomeningocele. Horm Res. 2001; 56:19–24. [PubMed: 11815723]

Ueno N, Greene NDE. Planar cell polarity genes and neural tube closure. Birth Def Res (Part C). 2003; 69:318–324.

van Meyel DJ, Sanchez-Sweatman OH, Kerkvliet N, et al. Genetic background influences timing, morphology and dissemination of lymphomas in p53-deficient mice. Int J Oncol. 1998; 13:917–922. [PubMed: 9772279]

Wang Y, Lian L, Golden JA, Morrisey EE, Abrams CS. PIP5KI gamma is required for cardiovascular and neuronal development. Proc Natl Acad Sci USA. 2007; 104:11748–11753. [PubMed: 17609388]

Wawersik S, Purcell P, Rauchman M, et al. BMP7 acts in murine lens placode development. Dev Biol. 1999; 207:176–188. [PubMed: 10049573]

Wilson MP, Hugge C, Bielinska M, Nicholas P, Majerus PW, Wilson DB. Neural tube defects in mice with reduced levels of inositol 1,3,4-trisphosphate 5/6-kinase. Proc Natl Acad Sci USA. 2009; 106:9831–9835. [PubMed: 19482943]

Ybot-Gonzalez P, Gaston-Massuet C, Girdler G, et al. Neural plate morphogenesis during mouse neurulation is regulated by antagonism of Bmp signaling. Development. 2007; 134:3203–3211. [PubMed: 17693602]

Yoshida K, Furuya S, Osuka S, et al. Targeted disruption of the mouse 3-phosphoglycerate dehydrogenase gene causes severe neurodevelopmental defects and results in embryonic lethality. J Biol Chem. 2004; 279:3573–3577. [PubMed: 14645240]

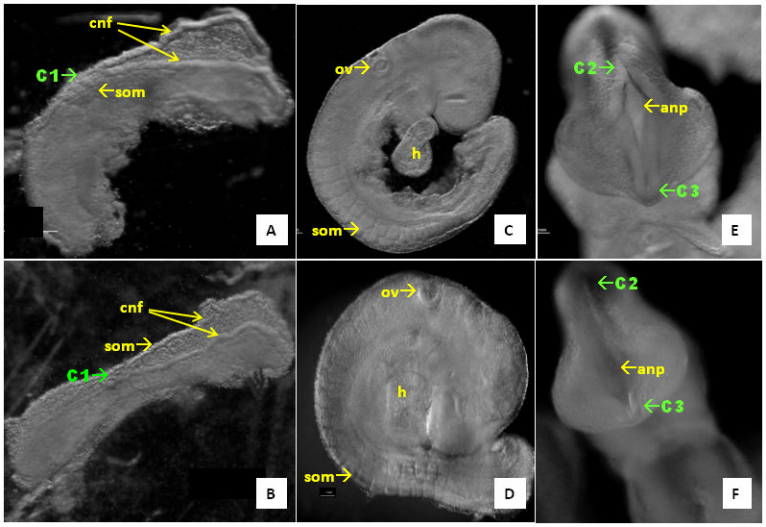

Figure 1. Comparison of neural tube development between C57BL6J and 129 embryos

(Ref: Copp, 2005). Dorsal view of a 129, E8.5 (A) and a C57BL6J, E8.5 whole embryo (B) showing closure point 1 (C1). Number of somites within E8.5 embryos from either strain is 5. E9.0 whole embryos: (c) 129 strain and (d) C57BL6J. Ventral view of a 129, E9.0 embryo (E) and a C57BL6J, E9.0 embryo (F), displaying closure point 2 (C2) and closure point 3 (C3). Number of somites within E9.0 embryos from either strain is 18-19. anp, anterior neuropore; cnf, cranial neural fold; h, heart; ov, otic vesicle; som, somite.

Table 1

Genes and ESTs Exhibiting Increased Expression in the E8.5 Neural Tube: C57BL6/J vs. 129P3[1]

Gene Title	Gene Abbreviations	Representative Public ID	Affymetrix Probe ID	Fold Change C57BL6/J vs. 129P3	P-value
EST		BG065719	1456319_at	268.88	0.003
3-phosphoglycerate dehydrogenase pseudogene; 3-phosphoglycerate dehydrogenase	Phgdh	AA561726	1454714_x_at	145.23	0.001
cDNA sequence BC005512 /// hypothetical protein LOC215866 /// hypothetical protein LOC629242 /// predicted gene, EG641366		AW763751	1435628_x_at	41.68	0.001
Ribosomal protein S9	Rps9	AA762498	1434624_x_at	40.82	0.002
Kinesin family member 5B	Kif5b	BI328541	1418429_at	30.72	0.002
cDNA sequence BC005512 /// hypothetical protein LOC215866 /// hypothetical protein LOC629242 /// predicted gene, EG641366		BC002257	142693 6_at	28.16	0.003
3-phosphoglycerate dehydrogenase pseudogene; predicted gene 9210; 3-phosphoglycerate dehydrogenase pseudogene; similar to 3-phosphoglycerate dehydrogenase; 3-phosphoglycerate dehydrogenase		BB204486	1456471_x_at	26.65	0.004
Acireductone dioxygenase 1	Adi1	AU046270	1438758_at	25.49	0.031
Myotubularin related protein 7	Mtmr7	BB431693	1447831_s_at	22.32	0.033
Hypothetical gene LOC72520	2610305J24Rik	AW215497	1428670_at	18.84	0.005
RIKEN cDNA A630033E08 gene; similar to A48830 probable transcription regulator NT fin12	Zfp945	BB391874	1437128_a_at	14.53	0.016
HAUS augmin-like complex, subunit 2	Haus2	BE686390	1430577_at	13.58	0.023
Lectin, mannose-binding, 1	Lman1	BE981934	144403 7_at	13.51	0.002
Ribosomal protein L17	Rpl17	BF453369	1453752_at	11.51	0.040
Galactosylceramidase	Galc	AK010101	1452907_at	11.24	0.001
RIKEN cDNA 9430027B09 gene	9430027B09Rik	AK020441	1454232_at	10.45	0.003
RIO kinase 3 (yeast)	Riok3	NM_024182	1460670_at	10.27	0.003
A kinase (PRKA) anchor protein 2 /// paralemmin 2 /// Palm2-Akap2 protein	Palm2	BB431157	1441055_at	9.93	0.045
Retinitis pigmentosa GTPase regulator interacting protein 1	Rpgrip1	NM_023879	1421144_at	9.65	0.004
EF hand domain containing 2	Efhd2	AA409309	1437478_s_at	8.59	0.035
Spermatogenesis associated 5-like 1	Spata5l1	AW215442	1455863_at	8.53	0.003

Birth Defects Res A Clin Mol Teratol. Author manuscript; available in PMC 2013 March 1.

Gene Title	Gene Abbreviations	Representative Public ID	Affymetrix Probe ID	Fold Change C57BL6/J vs. 129P3	P-value
Scm-like with four mbt domains 2	Sfmbt2	BM200222	1434353_at	7.95	0.005
Predicted gene, EG546524		BG078932	1448012_at	7.83	0.012
RIKEN cDNA 2010315B03 gene	2010315B03Rik	BB744779	1438238_at	7.55	0.050
EST (98% homology to a gene encoding a murine Type II ETn element)		BG976607	1434280_at	7.44	0.045
Zinc finger CCCH-type containing 4	Zc3h4	BG076273	1457458_at	7.39	0.001
UDP-Gal:betaGal beta 1,3-galactosyltransferase, polypeptide 6 /// similar to UDP-Gal:betaGal beta 1,3-galactosyltransferase, polypeptide 6	B3galt6	AV328064	1435252_at	7.22	0.007
Transcribed locus		BB368771	1442424_at	6.73	0.003
histone cluster 1, H4a; histone cluster 1, H4b; histone cluster 1, H4f; histone cluster 1, H4i histone cluster 1, H4m		BC019757	1424854_at	6.29	0.020
Mus musculus, clone IMAGE:6394389, mRNA	Sox11	BB656631	1431225_at	6.26	0.010
PEST proteolytic signal containing nuclear protein	Pcnp	BG067396	145273 5_at	5.64	0.011
C-type lectin domain family 1, member b	Clec1b	NM_019985	1421182_at	5.59	0.035
Peroxiredoxin 2	Prdx2	AK011963	1430979_a_at	5.51	0.015
RIKEN cDNA 3930401B19 gene /// RIKEN cDNA 1200016E24 gene /// RIKEN cDNA A130040M12 gene /// RIKEN cDNA E430024C06 gene		AU018141	1453238_s_at	5.35	0.022
Fucosyltransferase 10	Fut10	AV309082	1437388_at	4.86	0.031
Zinc finger protein 111	Zfp111	BB794862	1457185_at	4.85	0.015
Transcription termination factor 1	Ttf1	NM_009442	1420754_at	4.66	0.020
Leucine zipper transcription factor-like 1	Lztfl1	BB700884	1435514_at	4.63	0.019
Double homeobox B-like	Duxbl	AV321065	1445710_x_at	4.48	0.006
predicted gene 10393		BB609699	1452590_a_at	4.41	0.031
RIKEN cDNA C330024D12 gene	Eme2	AV245208	1460628_at	4.36	0.021
Budding uninhibited by benzimidazoles 1 homolog (S. cerevisiae)	Bub1	BB479886	1438571_at	4.35	0.014
Thioredoxin-like 4A	Txnl4a	NM_025299	1419179_at	4.21	0.035
Leucyl-tRNA synthetase, mitochondrial	Lars2	BB773089	1435682_at	3.97	0.015
RIKEN cDNA 3110045C21 gene	3110045C21Rik	AK014177	1430401_at	3.91	0.022

Gene Title	Gene Abbreviations	Representative Public ID	Affymetrix Probe ID	Fold Change C57BL6/J vs. 129P3	P-value
RIKEN cDNA 1810037I17 gene	1810037I17Rik	BC002135	1424365_at	3.91	0.001
Serine incorporator 3	Serinc3	BM244064	1434548_at	3.86	0.020
Serine hydroxymethyltransferase 1 (soluble)	Shmt1	AF237702	1425177_at	3.59	0.003
Growth factor, erv1 (S. cerevisiae)-like (augmenter of liver regeneration)	Gfer	BI901126	1452272_a_at	3.44	0.035
Transducin-like enhancer of split 1, homolog of Drosophila E(spl)	Tle1	NM_011599	142275 1_at	3.42	0.022
WAP four-disulfide core domain 2	Wfdc2	AF334269	142435 1_at	3.36	0.033
Dynein light chain LC8-type 1	Dynll1	BM939312	1440278_at	3.17	0.015
Double homeobox B-like		AK004227	1429099_at	3.08	0.002
Transmembrane protein 66	Tmem66	BC022616	142403 9_at	3.02	0.048
Tetratricopeptide repeat domain 8	Ttc8	BC017523	1424410_at	2.99	0.024
RIKEN cDNA C330011K17 gene	Zfp874a	BB398891	1434171_at	2.92	0.002
Fucosyltransferase 10	Fut10	BG067296	1454924_at	2.81	0.031
Rho-related BTB domain containing 3	Rhobtb3	BG801497	142966 1_at	2.81	0.030
Processing of precursor 1, ribonuclease P/MRP family, (S. cerevisiae)	Pop1	BG073302	142845 8_at	2.77	0.004
Zinc finger protein 593	Zfp593	AV214133	1447703_x_at	2.76	0.008
GATA zinc finger domain containing 2A	Gatad2a	AI840824	1455505_at	2.71	0.042
RIKEN cDNA 4930427A07 gene	4930427A07Rik	BE951637	1455818_at	2.71	0.028
DnaJ (Hsp40) homolog, subfamily A, member 2	Dja2	BB324466	1457233_at	2.70	0.027
Similar to polycomb group ring finger 5		BF660283	1434666_at	2.69	0.024
DPH5 homolog (S. cerevisiae)	Dph5	BG229936	1439049_at	2.65	0.002
Rho-related BTB domain containing 3	Rhobtb3	AV047988	1447869_x_at	2.61	0.001
Optic atrophy 3 (human)	Opa3	BB324282	1447724_x_at	2.60	0.003
Anterior pharynx defective 1b homolog (C. elegans)	Aph1b	BM219801	1435793_at	2.56	0.021
Zinc finger protein 39	Zfp39	BB311524	1441198_at	2.54	0.009
Shisa homolog 4 (Xenopus laevis)	Shisa4	BF468228	1438426_at	2.38	0.010
Zinc finger, CCHC domain containing 3	Zcchc3	AV140894	1428402_at	2.34	0.005
Phospholipase A2, group IVB (cytosolic) /// hypothetical protein		BC016255	1425045_at	2.27	0.036

Gene Title	Gene Abbreviations	Representative Public ID	Affymetrix Probe ID	Fold Change C57BL6/J vs. 129P3	P-value
LOC433466					
Phospholipase A2, activating protein	Plaa	BB532258	1444647_at	2.23	0.006
D-2-hydroxyglutarate dehydrogenase	D2hgdh	BB222646	1437840_s_at	2.21	0.011
Ribosomal protein S6 kinase, polypeptide 1	Rps6kb1	AI451506	1460705_at	2.13	0.047
RIKEN cDNA 2810417H13 gene	2810417H13Rik	AK017673	1419152_at	2.12	0.020
Sec23 interacting protein	Sec23ip	AW546839	1433627_at	2.08	0.005
RIKEN cDNA 4922501C03 gene	4922501C03Rik	BE848415	144273 3_at	2.08	0.049
RAB, member of RAS oncogene family-like 4	Ift27	AI413098	1434299_x_at	1.99	0.003
RNA binding motif protein 28	Rbm28	BM228459	1452091_a_at	1.89	0.025
Receptor interacting protein kinase 5	Dstyk	BB435342	1436301_at	1.88	0.033
Chloride intracellular channel 4 (mitochondrial)	Clic4	BB398988	1423393_at	1.87	0.002
RIKEN cDNA 2310008H09 gene	2310008H09Rik	BB452927	1436541_at	1.85	0.050
Olfactomedin-like 3	Olfml3	NM_133859	1448475_at	1.82	0.023
C1q domain containing 2	Fam132a	NM_026125	1417393_a_at	1.78	0.008
Proviral integration site 1	Pim1	AI323550	1435458_at	1.69	0.022
G protein-coupled receptor 180	Gpr180	NM_021434	1417245_at	1.59	0.029
EST	Epb4.1l4b	BB801576	1456570_at	1.58	0.004
Methyltransferase like 7A1	Mettl7a1	AV171622	1454858_x_at	1.52	0.044

[1]Quadruplicate gene expression data sets from the developing neural tubes of E8.5, C57BL6/J and 129P3 embryos. Only those genes and ESTs which demonstrated a statistically significant ($p < 0.05$) ***increase*** in expression of at least 1.5-fold in all four biological replicates (n=4) are included in this table. It is to be noted here that C57BL6/J vs. 129P3 means that expression in 129P3 was utilized as the baseline.

Table 2

Genes and ESTs Exhibiting Decreased Expression in The E8.5 Neural Tube: C57BL6/J vs. 129P3[1]

Gene Title	Gene Abbreviations	Representative Public ID	Affymetrix Probe ID	Fold Change C57BL6/J vs. 129P3	P-value
Superkiller viralicidic activity 2-like 2 (S. cerevisiae)	Skiv2l2	BM208991	1447517 at	−81.39	0.015
Mitogen-activated protein kinase 8	Mapk8	BB184171	1457936_at	−57.43	0.012
Phosphatidylinositol 4-kinase type 2 beta	Pi4k2b	NM_028744	1420411_a_at	−26.85	0.003
Predicted gene 13138; predicted gene 13242; hypothetical protein LOC100048814; reduced expression 2; zinc finger protein 600		BM198106	1438237_at	−22.87	0.005
Transcribed locus, moderately similar to NP_001013091.1 BTB (POZ) domain containing 9 [Rattus norvegicus]		BM233846	1458719_at	−20.56	0.024
TSC22 domain family, member 1	Tsc22d1	AW413169	1447360_at	−18.19	0.018
RNA binding motif protein 39	Rbm39	BB436856	1446147_at	−9.84	0.006
RNA binding motif protein 39	Rbm39	BB436856	1446148_x_at	−9.37	0.022
SRY-box containing gene 11	Sox11	BG072739	1436790_a_at	−8.63	0.027
Integrin alpha 9	Itga9	NM_133721	1460285_at	−8.54	0.022
Transmembrane protein 87A	Tmem87a	BC027354	1424454_at	−8.12	0.042
Tyrosine 3-monooxygenase/tryptophan 5-monooxygenase activation Protein, zeta polypeptide	Ywhaz	AV027921	1416103_at	−8.04	0.038
Arrestin domain containing 3	Arrdc3	AW556597	1459253_at	−7.40	0.007
Guanine nucleotide binding protein (G protein), beta 4	Gnb4	BI713933	1419469_at	−6.75	0.050
Transcribed locus		BB233975	1446140_at	−6.23	0.008
cDNA sequence BC023969	BC023969	BI664409	1445226_at	−6.16	0.029
Sec23 interacting protein	Sec23ip	BE685845	1439882_at	−5.53	0.003
HD domain containing 3	Hddc3	AW259452	1428692_at	−5.30	0.003
Syndecan 4	Sdc4	BC005679	1448793_a_at	−5.30	0.044
Pituitary tumor-transforming 1	Pttg1	AF069051	1424105_a_at	−5.28	0.025
CCR4-NOT transcription complex, subunit 7	Cnot7	AK007767	1430519_a_at	−4.97	0.013
Heme binding protein 1	Hebp1	AF117613	1418172_at	−4.93	0.050
PC4 and SFRS1 interacting protein 1	Psip1	BB074968	1442148_at	−4.89	0.019

Birth Defects Res A Clin Mol Teratol. Author manuscript; available in PMC 2013 March 1.

Gene Title	Gene Abbreviations	Representative Public ID	Affymetrix Probe ID	Fold Change C57BL6/J vs. 129P3	P-value
Catechol-O-methyltransferase	Comt	NM_007744	1418701_at	−4.89	0.043
Dishevelled associated activator of morphogenesis 1	Daam1	AW988556	1431035_at	−4.46	0.047
FSHD region gene 1	Frg1	NM_013522	1417253_at	−4.21	0.005
RIKEN cDNA A630033E08 gene	Zfp945	BB391874	1437127_at	−4.03	0.011
RIKEN cDNA 1500011B03 gene	1500011B03Rik	BB782615	1456857_at	−3.99	0.006
Secreted frizzled-related protein 1	Sfrp1	BI658627	1448395_at	−3.74	0.022
Glyoxalase 1	Glo1	BC024663	1424109_a_at	−3.57	0.017
CAP, adenylate cyclase-associated protein 1 (yeast)	Cap1	NM_007598	1417461_at	−3.50	0.011
Phenylalanyl-tRNA synthetase, beta subunit	Farsb	AK012154	1430986_at	−3.24	0.022
Solute carrier family 38, member 9	Slc38a9	BQ031896	1436456_at	−3.19	0.014
Histidyl-tRNA synthetase	Hars	BC020088	1417024_at	−3.06	0.022
histone cluster 1, H3a; histone cluster 1, H3b; histone cluster 1, H3c; histone cluster 1, H3d; histone cluster 1, H3e; histone cluster 1, H3f; histone cluster 1, H3g; histone cluster 1, H3h; histone cluster 1, H3i; histone cluster 2, H3b; histone cluster 2, H3c1; histone cluster 2, H3c2		NM_019469	1460314_s_at	−2.88	0.001
Zinc finger protein 286	Zfp286	BE651907	1425080_at	−2.86	0.000
Expressed sequence AI848218	Slc38a9	AW542748	1455612_at	−2.76	0.028
RIKEN cDNA 5730437N04 gene	5730437N04Rik	BC019420	1424045_at	−2.76	0.009
Tripartite motif-containing 68	Trim68	AW493298	1455124_at	−2.74	0.000
Pituitary tumor-transforming 1	Pttg1	NM_013917	1419620_at	−2.63	0.011
LanC (bacterial lantibiotic synthetase component C)-like 1	Lancl1	AJ294535	1427012_at	−2.62	0.046
Pituitary tumor-transforming 1	Pttg1	AV105428	1438390_s_at	−2.62	0.013
Predicted gene 11277; predicted gene 13646; histone cluster 1, H2bc; histone cluster 1, H2be; histone cluster 1, H2bl; histone cluster 1, H2bm; histone cluster 1, H2bp; similar to Hist1h2bj protein		M25487	1452540_a_at	−2.48	0.035
BCNP1 homolog	Fam129c	BB763642	1457728_at	−2.46	0.001
Transcribed locus		AI506321	1458585_at	−2.44	0.022
Enhancer of yellow 2 homolog (Drosophila)	Eny2	AI595744	1429410_at	−2.38	0.008
ERGIC and golgi 3	Ergic3	BB556862	1451017_at	−2.25	0.023

Gene Title	Gene Abbreviations	Representative Public ID	Affymetrix Probe ID	Fold Change C57BL6/J vs. 129P3	P-value
RIO kinase 3 (yeast)	Riok3	NM_024182	1422650_a_at	−2.22	0.033
Importin 9	Ipo9	AF273672	1424466_at	−2.20	0.026
NIMA (never in mitosis gene a)-related expressed kinase 3	Nek3	NM_011848	1418947_at	−2.18	0.040
Coiled-coil domain containing 117	Ccdc117	AV108872	1452218_at	−2.17	0.037
Serum response factor binding protein 1 /// similar to SRF-dependent transcription regulation associated protein		BB041813	1420510_at	−2.15	0.043
ATPase, H+ transporting, lysosomal V1 subunit G1	Atp6v1g1	BI154058	1423255_at	−2.12	0.036
Sulfatase modifying factor 2 /// similar to sulfatase modifying factor 2	Sumf2	BB822050	1429714_at	−2.11	0.011
YTH domain family 1	Ythdf1	BB350365	1415767_at	−2.09	0.000
Dihydrolipoamide S-acetyltransferase (E2 component of pyruvate dehydrogenase complex)	Dlat	AV336908	1452005_at	−2.06	0.009
Zinc finger protein 157	Zfp157	AK011480	1452945_at	−2.03	0.048
Germ cell-specific gene 2	Gsg2	BE457839	1450886_at	−2.00	0.004
RIKEN cDNA 1500035H01 gene	Ift46	NM_023831	1417474_at	−1.97	0.004
Importin 9	Ipo9	C78347	1441645_s_at	−1.96	0.022
Transmembrane protein 181 /// similar to G protein-coupled receptor 178		BB309117	1435948_at	−1.93	0.050
Fucosidase, alpha-L- 1, tissue	Fuca1	NM_024243	1416109_at	−1.76	0.000
Suppressor of Ty 16 homolog (S. cerevisiae)	Supt16h	AW536705	1419741_at	−1.67	0.003
Histone cluster 1, H2bp	Hist1h2bp	M25487	1427762_x_at	−1.65	0.026
EST		BB486980	1459618_at	−1.61	0.017
WAS protein family, member 2	Wasf2	BM207372	1454673_at	−1.59	0.005
Fusion, derived from t(12;16) malignant liposarcoma (human)	Fus	AF224264	1451285_at	−1.55	0.018
Similar to WW domain-containing adapter protein with coiled-coil	Wac	BB822150	1439249_at	−1.51	0.050

[1]Quadruplicate gene expression data sets from the developing neural tubes of E8.5, C57BL6/J and 129P3 embryos. Only those genes and ESTs which demonstrated a statistically significant ($p < 0.05$) ***decrease*** in expression of at least 1.5-fold in all four biological replicates (n=4) are included in this table. It is to be noted here that C57BL6/J vs. 129P3 means that expression in 129P3 was utilized as the baseline.

Table 3

Verification of GeneChip Microarray Data by TaqMan Quantitative Real-Time PCR[1]

Gene[2]	Affymetrix Probe ID#	Microarray	TaqMan	[3]Concordance
D-3-phosphoglycerate dehydrogenase (Phgdh)	1456471_x_at	+26.70	+34.00	+/+
EST: similar to KRAB box containing protein, NT fin12	1437128_a_at	+14.50	+14.00	+/+
Galactosylceramidase	1452907_at	+11.23	+2.10	+/+
UDP-Gal:betaGal beta 1,3-galactosyltransferase, polypeptide 6	1442424_at	+7.22	+21.00	+/+
SRY-box containing gene 11	1436790_a_at	−8.62	−1.62	+/+
Transducin-like enhancer of split 1, homolog of Drosophila E(spl)	1422751_at	+3.42	−1.53	+/−
Rho-related BTB domain containing-3	1429661_at	+2.81	+1.55	+/+
Importin-9	1424466_at	−2.20	−1.60	+/+
Secreted frizzled-related protein 1	1448395_at	−3.74	−2.55	+/+
Dishevelled associated activator of morphogenesis 1	1431035_at	−4.45	−9.51	+/+
TSC22 domain family, member 1	1447360_at	−18.20	−11.13	+/+
Mitogen-activated protein kinase 8 (JNK-1)	1457936_at	−57.42	−33.03	+/+

[1]Level of expression of 12 genes in E8.5 developing neural tube from C57BL6/J and 129P3 embryos were compared using Affymetrix GeneChip Arrays and TaqMan Quantitative Real-Time PCR as detailed in Materials and Methods. Analysis was performed on 2-3 independent sets of cDNA and each cDNA sample was tested in duplicate. Statistical significance was determined by one-way ANOVA followed by Bonferroni's Multiple Comparison Test, using GraphPad Prism, v. 4.02 (GraphPad Software, Inc., San Diego, CA). P-values of <0.05 were considered significant.

[2]Target genes were selected based on results from Affymetrix GeneChip Arrays.

[3]+/+ indicates full concordance in the level of gene expression obtained using Affymetrix GeneChip Arrays and TaqMan Quantitative Real-Time PCR. "+/−" indicates a differing level of gene expression was detected in the E8.5 developing neural tubes using Affymetrix GeneChip Arrays and TaqMan Quantitative Real-Time PCR. .